inibition of DNA binding bit not for cytoplasmic retention of c-Rel or RelA homodimers. *Mol. Cell. Biol.* **15,** 872–882 (1995).

Acknowledgements

We are grateful to A. Phillips, M. Dobrovolskaia and D. Woods for helpful discussion. We thank C. Rosen, G. Nunez, A. Israel and E. Harlow for plasmids, and D. Baltimore for the p65-deficient MEFs. We are also indebted to S. Lowe for providing us with E1A-expressing retroviruses.

Correspondence and requests for materials should be addressed to K.V. (e-mail: vousden@ncifcrf.gov).

Interplay of p53 and DNA-repair protein XRCC4 in tumorigenesis, genomic stability and development

Yijie Gao*†, David O. Ferguson*†‡, Wei Xie*, John P. Manis*, JoAnn Sekiguchi*, Karen M. Frank*, Jayanta Chaudhuri*, James Horner§, Ronald A. DePinho§ & Frederick W. Alt*

** Howard Hughes Medical Institute, The Children's Hospital, and Centre for Blood Research, and Department of Genetics, Harvard Medical School, Boston, Massachusetts 02115, USA*
‡ Department of Pathology, Brigham and Women's Hospital, Boston, Massachusetts 02115, USA
§ Departments of Adult Oncology, Medicine and Genetics, Harvard Medical School and Dana Farber Cancer Institute, 44 Binney Street, Boston, Massachusetts 02115, USA
† These authors contributed equally to this work

XRCC4 is a non-homologous end-joining protein employed in DNA double strand break repair and in V(D)J recombination[1,2]. In mice, XRCC4-deficiency causes a pleiotropic phenotype, which includes embryonic lethality and massive neuronal apoptosis[2]. When DNA damage is not repaired, activation of the cell cycle checkpoint protein p53 can lead to apoptosis[3]. Here we show that p53-deficiency rescues several aspects of the XRCC4-deficient phenotype, including embryonic lethality, neuronal apoptosis, and impaired cellular proliferation. However, there was no significant rescue of impaired V(D)J recombination or lymphocyte development. Although p53-deficiency allowed postnatal survival of XRCC4-deficient mice, they routinely succumbed to pro-B-cell lymphomas which had chromosomal translocations linking amplified c-myc oncogene and IgH locus sequences. Moreover, even XRCC4-deficient embryonic fibroblasts exhibited marked genomic instability including chromosomal translocations. Our findings support a crucial role for the non-homologous end-joining pathway as a caretaker of the mammalian genome, a role required both for normal development and for suppression of tumours.

Cellular DNA double strand breaks (DSBs) result from oxidative metabolism, exogenous damaging agents, or endonuclease activity[4]. Mammalian cells repair these potentially lethal or oncogenic chromosomal lesions either by non-homologous end-joining (NHEJ) in which broken DNA ends are ligated directly[5] or by homologous recombination employing a template of similar sequence[6]. The early lymphocyte-specific V(D)J recombination reaction is initiated by DSBs made by RAG endonuclease[7]. Subsequently, V(D)J recombination is completed by the ubiquitous NHEJ components, including the Ku70 and Ku80 DNA end-binding complex (Ku) and the DNA-dependent protein kinase catalytic subunit (DNA-PKcs), as well as XRCC4 and DNA Ligase IV (Lig4) which probably cooperate in ligation[4,5].

Mice deficient in XRCC4 (or Lig4) die during late embryonic development[2,8,9]. XRCC4-deficient embryos display extensive apoptotic death of newly generated, postmitotic neurons throughout the developing nervous system[2]. In addition, progenitor (pro)-lymphocyte development is arrested due to impaired V(D)J recombination. XRCC4-deficient embryos are also growth-retarded and their fibroblasts exhibit decreased proliferation and premature senescence in culture[2]. The precise cause of embryonic death is unknown, but the massive apoptotic neuronal phenotype is associated with defective NHEJ and may be a checkpoint response to eliminate nascent neurons with DSBs that have not been repaired[10]. Normally, DSBs lead to stabilization and activation of p53, followed by cell cycle arrest or apoptosis depending on cell type and/or physiological context[3].

Mice containing a mutation that inactivates the *p53* gene (either heterozygous, $p53^{+/-}$, or homozygous, $p53^{-/-}$) are relatively normal, though $p53^{-/-}$ mice become cancer-prone at about 5 months of age[3]. To test potential involvement of p53 in XRCC4-deficient phenotypes, we bred $XRCC4^{+/-}$ mice with $p53^{-/-}$mice and then bred progeny to generate the various $XRCC4^{-/-}$ cohorts against all three p53 genotypes. We have not observed a live $XRCC4^{-/-}$

a

Genotype	$XR^{+/-}$ $p53^{+/-}$	$XR^{+/-}$ $p53^{-/-}$	$XR^{+/-}$ $p53^{+/+}$	$XR^{-/-}$ $p53^{+/+}$	$XR^{-/-}$ $p53^{+/-}$	$XR^{-/-}$ $p53^{-/-}$
Expected	60	81	14	7	44	47
Actual	88	74	10	0	17	33

b

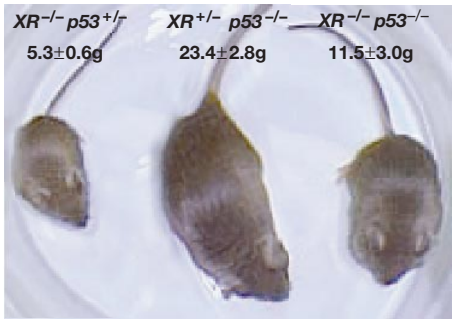

c

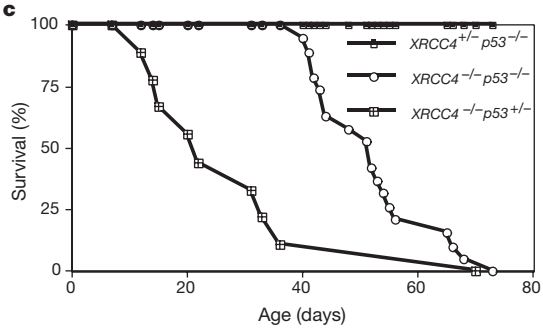

Figure 1 Effects of p53-deficiency on survival of $XRCC4^{-/-}$ mice. **a**, p53 deficiency rescues embryonic lethality. Genotypes of offspring from $XRCC4^{+/-}p53^{+/-} \times XRCC4^{+/-}p53^{+/-}$, $XRCC4^{+/-}p53^{+/-} \times XRCC4^{+/-}p53^{-/-}$, and $XRCC4^{+/-}$ $p53^{-/-} \times XRCC4^{+/-}$ $p53^{-/-}$ crosses. Shown are relevant genotypes for $XRCC4^{+/-}$ and $XRCC4^{-/-}$ offspring. 11 pups died within 2 days of birth without genotyping and were not included. **b**, Average weights of 5-week-old $XRCC4^{-/-}p53^{+/-}$ ($n = 3$), $XRCC4^{+/-}$ $p53^{-/-}$ ($n = 10$) and $XRCC4^{-/-}p53^{-/-}$ ($n = 10$) mice and a representative photograph of littermates. **c**, Percentage survival of $XRCC4^{+/-}p53^{-/-}$ ($n = 30$), $XRCC4^{-/-}$ $p53^{+/-}$ ($n = 9$) and $XRCC4^{-/-}$ $p53^{-/-}$ ($n = 19$) mice versus age (in days). 95% of $XRCC4^{-/-}p53^{-/-}$ mice developed pro-B ($B220^{+}CD43^{+}CD4^{-}CD8^{-}Thy1^{-}$) lymphomas. $XRCC4^{+/-}$ data points represent the death or killing of terminally ill mice. XR, XRCC4.

$p53^{+/+}$ mouse, but $XRCC4^{-/-}p53^{-/-}$ mice were born at nearly the predicted Mendelian frequency ($P = 0.3$), indicating rescue of $XRCC4^{-/-}$ embryonic lethality by p53-deficiency (Fig. 1a). Moreover, p53 haplo-insufficiency ($p53^{+/-}$) also rescued embryonic lethality, albeit at reduced frequency ($P = 0.05$, Fig. 1a). Both $XRCC4^{-/-}p53^{-/-}$ and $XRCC4^{-/-}p53^{+/-}$ mice were growth-retarded, although this defect was more severe in the latter (Fig. 1b).

To investigate whether increased neuronal death in XRCC4-deficient embryos resulted from a p53-dependent process, we conducted a detailed histological analysis of the central nervous system (CNS) of $XRCC4^{-/-}p53^{-/-}$ and $XRCC4^{-/-}p53^{+/-}$ embryos at embryonic day (E) 12.5–E13.5, the stage at which the $XRCC4^{-/-}$ neuronal phenotype is most pronounced. Deficiency of p53 completely rescued the apoptotic phenotype of $XRCC4^{-/-}$ neurons, as we observed similar, low levels of pyknosis throughout the developing CNS of $XRCC4^{-/-}p53^{-/-}$ and $XRCC4^{+/+}p53^{+/+}$ embryos, in contrast with the high levels in $XRCC4^{-/-}p53^{+/+}$ embryos (Fig. 2a). We also observed a marked, but not complete, attenuation of apoptosis in the $XRCC4^{-/-}p53^{+/-}$CNS (Fig. 2a).

Impaired lymphocyte development in $XRCC4^{-/-}$ embryos occurs at the $CD4^-CD8^-$ (DN) pro-T cell stage and the $B220^+CD43^+$ pro-B-cell stage[2]. We did not observe rescue of bone marrow B-cell development beyond the $B220^+CD43^+$stage in postnatal $XRCC4^{-/-}p53^{-/-}$ or $XRCC4^{-/-}p53^{+/-}$ mice, but $B220^+CD43^+$ cell numbers appeared moderately increased in $XRCC4^{-/-}p53^{-/-}$ compared with $XRCC4^{-/-}p53^{+/-}$ mice (data not shown). Likewise, total $XRCC4^{-/-}p53^{-/-}$ or $XRCC4^{-/-}p53^{+/-}$ thymocyte numbers remained very low at 4 weeks; although there was a very small population of $CD4^+CD8^+$ (DP) cells in $XRCC4^{-/-}p53^{-/-}$ thymuses (Fig. 2b). However, as most $XRCC4^{-/-}p53^{-/-}$ DP cells lacked detectable cytoplasmic TCRβ expression (data not shown), they were probably generated by "nonspecific" p53-related processes like those observed in $p53^{-/-}RAG^{-/-}$mice[11]. In $XRCC4^{-/-}$ thymuses, the most immature DN thymocyte populations ($CD44^+CD25^-$ and $CD44^+CD25^+$) were

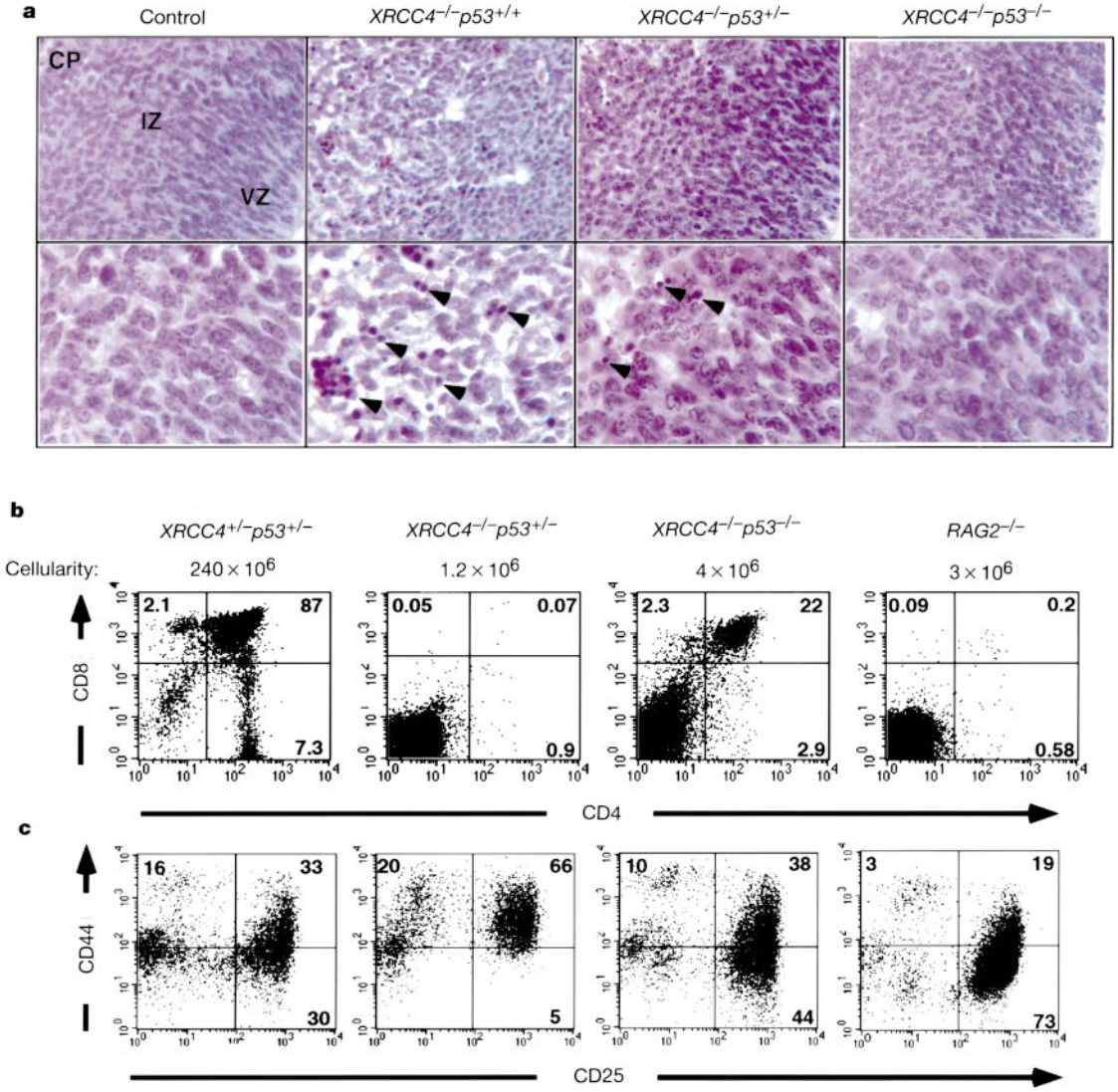

Figure 2 Effects of p53 deficiency on developing $XRCC4^{-/-}$ neurons and T cells. **a**, Histological analysis of $XRCC4^{+/+}p53^{-/-}$, $XRCC4^{-/-}p53^{+/-}$, $XRCC4^{-/-}p53^{-/-}$ and $XRCC4^{-/-}p53^{+/+}$embryonic CNS. Haematoxylin and eosin stained sections (5 μm) from comparable regions in the developing cerebral cortex (E13.5) are shown. Arrows indicate pyknotic nuclei. VZ, ventricular zone; IZ, intermediate zone; CP, cortical plate. Original magnification: x400 and x1,000. **b**, CD4 and CD8 profile of thymocytes from 4-week-old $XRCC4^{+/-}p53^{+/-}$, $XRCC4^{-/-}p53^{+/-}$, $XRCC4^{-/-}p53^{-/-}$ and $RAG2^{-/-}$ mice. Thymic cellularity is shown above fluorescence-activated cell sorting (FACS) plots. **c**, CD25 and CD44 profile of $CD4^-CD8^-$ (DN) T cells from $XRCC4^{+/-}p53^{+/-}$, $XRCC4^{-/-}p53^{+/-}$, $XRCC4^{-/-}p53^{-/-}$ and $RAG2^{-/-}$ fetal thymuses. E16.5 fetal thymocytes were triple-stained with: (1) an equal titre mixture of cytochrome C-conjugated antibodies against CD4, CD8, CD3, B220, CD19, Gr-1, Mac-1; (2) FITC-anti-CD25; and (3) PE-anti-CD44. Cells negative for the first set (1) were plotted for CD25 versus CD44. FITC, fluorescein isothiocyanate; PE, phycoerythrin.

comparable to those of controls; while the more mature $CD44^-$ $CD25^+$ DN population (which undergoes TCRβ rearrangement) was nearly absent due to cell death induced by unrepaired RAG-generated DSBs[2,12,13] (Fig. 2c). The $CD44^-CD25^+$ DN population was restored in *XRCC4*$^{-/-}$*p53*$^{-/-}$, but not *XRCC4*$^{-/-}$*p53*$^{+/-}$, thymuses (Fig. 2c).

XRCC4$^{-/-}$*p53*$^{-/-}$ and *XRCC4*$^{-/-}$*p53*$^{+/-}$ mice had substantially shorter lifespans than wild-type mice or *p53*$^{-/-}$ controls (Fig. 1c). *XRCC4*$^{-/-}$*p53*$^{+/-}$ mice generally died within the first 3–4 postnatal weeks, potentially from nutritional problems. In contrast, most *XRCC4*$^{-/-}$*p53*$^{-/-}$ mice appeared healthy until postnatal week 6; but then became moribund with widely disseminated pro-B-cell lymphomas (Fig. 1c). Spectral Karyotyping (SKY; ref. 14) of two lymphomas (lymphomas 184 and 294) revealed non-reciprocal translocations between chromosomes 12 and 15 (Fig 3a), potentially implicating the IgH (chromosome 12) and c-myc loci (chromosome 15). Chromosomal fluorescence *in situ* hybridization (FISH) analyses on lymphoma 294 confirmed IgH and c-myc co-localization, and indicated co-amplification based on the greatly increased area and intensity of each signal compared to single copy signals (Fig. 3b). Both Southern blotting and quantitative polymerase chain reaction (PCR) confirmed c-myc gene amplification (7- to 16-fold) in five of six tumours analysed. The sixth (lymphoma 184), had an alteration within or near the c-myc gene (Fig. 3c and data not shown). Southern analyses were consistent with classically large amplicons, as there was amplification of sequences lying 200 kilobases (kb) 3′ of the IgH J_H-region (HS3a) in all c-myc-amplified tumours, and amplification of rearranged J_H-region sequences in a subset of the c-myc-amplified tumours (Fig. 3b). Lack of amplified J_H sequences in some c-myc/HS3a-amplified lymphomas probably reflects deletion of the J_H region before or during the translocation/amplification process.

XRCC4$^{-/-}$mouse embryonic fibroblasts (MEFs) exhibit prolonged doubling times and premature senescence, but retain normal cell cycle checkpoints[2]. However, *XRCC4*$^{-/-}$*p53*$^{-/-}$ MEFs, in contrast to *XRCC4*$^{-/-}$*p53*$^{+/-}$ or *XRCC4*$^{-/-}$*p53*$^{+/+}$ MEFs, doubled more rapidly (after a lag) than wild-type MEFs (Fig. 4a). The *p53*$^{-/-}$ genotype also rescued premature senescence of *XRCC4*$^{-/-}$ MEFs in continuous passage assays (data not shown). Furthermore, bromodeoxyuridine (BrdU) incorporation assays revealed a similar proportion of cycling MEFs in *XRCC4*$^{-/-}$*p53*$^{-/-}$ and *p53*$^{-/-}$ controls; whereas *XRCC4*$^{-/-}$*p53*$^{+/+}$ and *XRCC4*$^{-/-}$*p53*$^{+/-}$ cultures contained fewer cycling cells (Fig. 4c). Thus, p53-deficiency rescues growth defects and premature senescence, allowing XRCC4-deficient cells to progress through the cell cycle. Finally, transient transfection assays demonstrated that, like *XRCC4*$^{-/-}$*p53*$^{+/+}$ cells[2], *XRCC4*$^{-/-}$*p53*$^{-/-}$ MEFs were severely impaired for V(D)J coding and signal join formation (data not shown).

Ku-deficiency leads to chromosomal fragmentation and related anomalies[15]. However, the consistent appearance of pro-B lymphomas with IgH/c-myc translocations in *XRCC4*$^{-/-}$*p53*$^{-/-}$ mice suggested that NHEJ deficiency might also promote translocations catalysed via an alternative repair pathway. To test for a more global XRCC4-deficient translocation phenotype, we examined karyotypic instability in *XRCC4*$^{-/-}$ MEFs using SKY. No anomalies were observed in 31 wild-type MEF metaphases. However, out of 20

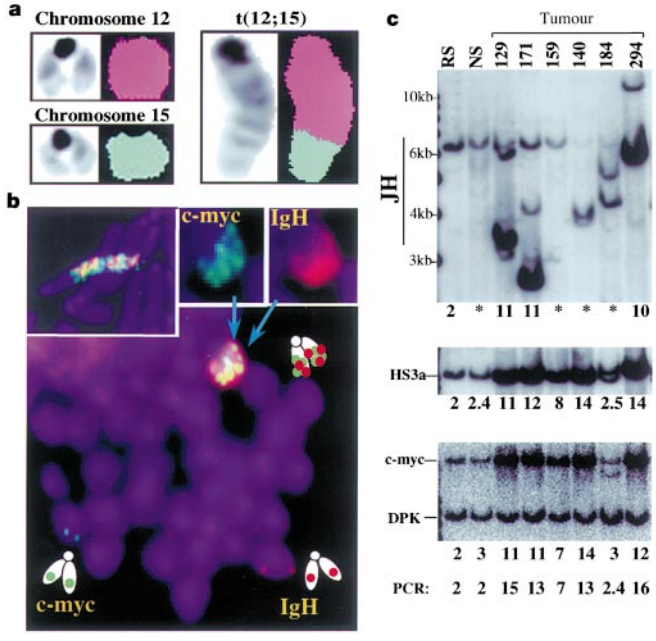

Figure 3 IgH and c-myc gene alterations in *XRCC4*$^{-/-}$*p53*$^{-/-}$ pro-B-cell lymphomas. **a**, Spectral Karyotyping (SKY) of *XRCC4*$^{-/-}$*p53*$^{-/-}$ lymphoma cells reveals a clonal non-reciprocal translocation involving chromosomes 12 (pink) and 15 (green) (right; t(12;15)). Normal chromosomes 12 and 15 are shown on left. **b**, FISH analysis of lymphoma 294 metaphases. Upper right panels show c-myc (green) and Cμ (red) signals separately. Bottom, merged signals (yellow), and individual unaltered alleles (dots) located on individual chromatids. Top, left, merged signals in a different lymphoma 294 metaphase, highlighting amplification. **c**, Southern analyses of lymphoma DNA. *Eco*R1-digested DNA from *RAG2*$^{-/-}$ spleen (RS), *XRCC4*$^{+/-}$*p53*$^{-/-}$ spleen (NS), and *XRCC4*$^{-/-}$*p53*$^{-/-}$ lymphomas was probed with J_H (top), HS3a (middle) or c-myc plus DNA-PKcs (DPK, loading control) probe (bottom). Bold numbers, relative gene dosage based on setting RS control to 2. PCR, relative c-myc gene dosage assessed by quantitative fluorogenic PCR. Asterisk, quantitation of J_H dosage was performed only on bands amplified above the RS control level. HS3a-hyridizing doublets represent polymorphism between 129 and C57B/6 alleles.

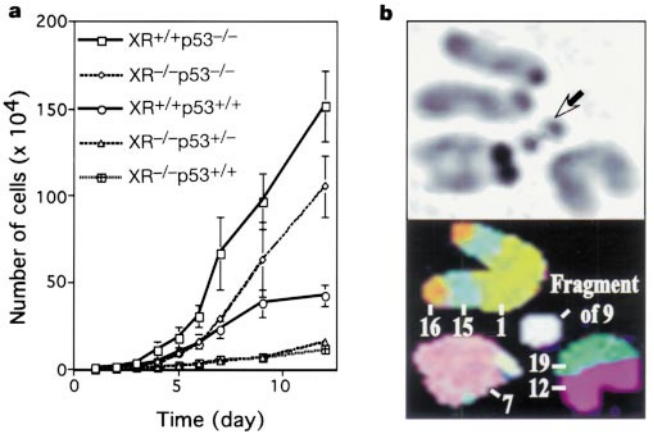

c

	XR+/+ p+/+	XR+/+ p+/−	XR+/+ p−/−	XR−/− p+/+	XR−/− p+/−	XR−/− p−/−
BrdU+(%) 50hr	86	91	99	55	79	98
BrdU+(%) 1hr	7.1	16.4	25.5	4.5	8.6	23

Figure 4 Growth analysis and cytogenetic studies of MEFs. **a**, Growth kinetics of *XRCC4*$^{-/-}$*p53*$^{-/-}$ and XRCC4$^{-/-}$p53$^{+/-}$ MEFs. Passage 1 (P1) MEFs (from three embryos of each genotype) were plated at 10^4 per well in replicate wells (6-well plates) and counted every 24 h. **b**, Portion of a metaphase from cultured *XRCC4*$^{-/-}$ MEFs. Top, 4,6-diamidino-2-phenylindole (DAPI) staining; bottom, SKY analysis. Two non-reciprocal translocations and a fragment involving indicated chromosomes are present, as well as a normal chromosome 7. **c**, Cell cycle analysis of MEFs. Asynchronous P3 MEFs were either cultured in the presence of BrdU for 50 h or pulsed for 1 h; the percentage of BrdU-positive ($BrdU^+$) cells is shown. XR, XRCC4; p, p53.

XRCC4$^{-/-}$ metaphases, three contained translocations (Fig. 4b), six had at least one acentric fragment, two had a detached centromere, and two had a short arm fusion. In total, 55% contained at least one anomaly.

We conclude that XRCC4 and, by extension, NHEJ is crucial for maintaining mammalian genomic stability. However, embryonic lethality, increased neuronal apoptosis and cellular proliferation defects of *XRCC4*$^{-/-}$ mice appear to result from a p53-dependent response to DNA damage that has not been repaired, as opposed to defective NHEJ *per se*. Thus, p53-deficiency permits survival of XRCC4-deficient embryos, accompanied by dramatic neuronal rescue, allowing generation of adult *XRCC4*$^{-/-}$*p53*$^{-/-}$ mice with a functional nervous system. In contrast, p53-deficiency does not substantially rescue lymphogenesis; probably because the *XRCC4*$^{-/-}$*p53*$^{-/-}$ lymphocyte progenitors still cannot efficiently assemble and express functional Ig and TCR genes needed to drive expansion and development. We conclude that the NHEJ requirements for lymphogenesis are more stringent than for neurogenesis, as development of a largely functional nervous system can occur in the absence of XRCC4. An intriguing question is whether or not *XRCC4*$^{-/-}$*p53*$^{-/-}$neurons become functional without repairing potentially broken DNA ends. While p53-deficiency also rescued growth and senescence defects in XRCC4-deficient MEFs, *XRCC4*$^{-/-}$*p53*$^{-/-}$ mice remained growth-retarded. Thus, growth deficiency appears to result from an XRCC4-dependent process distinct from that involved in the neuronal apoptosis or fibroblast growth-deficient phenotypes.

While p53 inactivation prolonged survival of XRCC4-deficient mice, it was at the expense of early susceptibility to pro-B-cell lymphomas with translocations/amplifications of c-myc and IgH loci. These findings support the notion that gene amplification may be enhanced by NHEJ-deficiency in the *p53*$^{-/-}$ background[16]. The tumour susceptibility phenotype of *XRCC4*$^{-/-}$*p53*$^{-/-}$ mice contrasts with that of *p53*$^{-/-}$ mice, which develop pro-T-cell lymphomas lacking translocations later in life[17,18]. Therefore, XRCC4-deficiency changes both the type and onset-time of tumours in a *p53*$^{-/-}$ background, reminiscent of the SCID (DNA-PKcs) mutation effect on p53-deficiency[12,13,17,19]. Ig/myc translocations are a frequent feature of certain human and murine B-cell malignancies[20], apparently resulting from aberrant V(D)J or class switch recombination. The high frequency of IgH/c-myc translocations in *XRCC4*$^{-/-}$*p53*$^{-/-}$ pro-B lymphomas may reflect continued cycling of NHEJ-deficient pro-B cells with RAG-initiated DSBs at the IgH locus, allowing aberrant recombination via secondary repair pathways[21] or RAG-mediated transpositions[22,23]. □

Methods

Generation of *XRCC4*$^{-/-}$*p53*$^{-/-}$ and *XRCC4*$^{-/-}$*p53*$^{+/-}$ mice

The *p53*$^{-/-}$ and *XRCC4*$^{+/-}$ mice described previously[2,24] were bred to generate *XRCC4*$^{+/-}$ *p53*$^{+/-}$ mice, which were either intercrossed or backcrossed with *p53*$^{-/-}$ mice to generate *XRCC4*$^{-/-}$*p53*$^{-/-}$, *XRCC4*$^{-/-}$*p53*$^{+/-}$, *XRCC4*$^{+/-}$ *p53*$^{+/-}$ and *XRCC4*$^{+/-}$ *p53*$^{-/-}$ mice. Genotypes were determined by Southern analyses of tail DNA. *P* values were calculated using the 2-tailed Fisher's Exact Test.

Preparation and analyses of MEFs

MEFs were prepared from E13.5 embryos as described[2]. MEFs prior to passage were designated passage 0 (P0), and subsequent passages as P1, P2, and so on, when grown to confluency and split at 1:5. Growth rates, senescence assays and cell cycle analyses were performed as described[2].

Flow Cytometry

Flow cytometry analysis was performed on single cell suspensions as described[2].

Southern analyses

Duplicate Southern blots of genomic DNA from control tissues or *XRCC4*$^{-/-}$*p53*$^{-/-}$tumour masses were probed either with a J_H probe followed by a DNA-PKcs probe, or with a c-myc probe, a DNA-PKcs probe, and a HS3a probe sequentially. A *Nae*I–*Eco*RI fragment from the J_H locus (between J4 and Eμ) was used as J_H probe, and an *Eco*RI–*Hin*dIII fragment from the region just 3′ to Cα was used as the HS3a probe. A c-myc complementary DNA fragment (exons 2 and 3) and a *Xba*I–*Hin*dIII fragment (exon 2 and 3) of the DNA-PKcs gene were used as probes.

Quantitative Fluorogenic PCR for c-myc Gene Amplification

Genomic c-myc sequences were quantified by real time PCR using a fluorogenic 5′ nuclease assay described previously[25]. The c-myc primers were from exon 1.

Chromosomal analysis

Lymphoma cultures grown overnight in the presence of IL-7 or passage 3–5 MEFs (1×10^6) were exposed to (100 ng ml^{-1}) Colcemid (GibcoBRL; KaryoMAX Colcemid solution) for 12 h (lymphomas) or 3 h (MEFs). Chromosomal aberrations were identified using SKY paint probes and an interferometer[14] (Applied Spectral Imageing, Carlsbad, CA) with a CCD camera mounted on a Nikon Eclipse microscope. Genomic probes for FISH analysis were nick-translated using biotin-11-dUTP or digoxigenin-16-dUTP by standard procedures (Boehringer-Mannheim). Hybridization was detected by anti-digoxigenin rhodamine or fluorescein-conjugated avidin (Boehringer-Mannheim). Images were obtained with a CCD camera interfaced with a Zeiss Axioskop microscope.

Received 5 February; accepted 17 March 2000.

1. Li, Z. *et al.* The XRCC4 gene encodes a novel protein involved in DNA double-strand break repair and V(D)J recombination. *Cell* **83,** 1079–1089 (1995).
2. Gao, Y. *et al.* A critical role for DNA end-joining proteins in both lymphogenesis and neurogenesis. *Cell* **95,** 891–902 (1998).
3. Levine, A. J. p53, the cellular gatekeeper for growth and division. *Cell* **88,** 323–331 (1997).
4. Jeggo, P. A. Identification of genes involved in repair of DNA double-strand breaks in mammalian cells. *Radiat. Res.* **150,** S80–91 (1998).
5. Lieber, M. R. The biochemistry and biological significance of nonhomologous DNA end joining: an essential repair process in multicellular eukaryotes. *Genes Cells* **4,** 77–85 (1999).
6. Takata, M. *et al.* Homologous recombination and non-homologous end-joining pathways of DNA double-strand break repair have overlapping roles in the maintenance of chromosomal integrity in vertebrate cells. *EMBO J.* **17,** 5497–5508 (1998).
7. Gellert, M. Recent advances in understanding V(D)J recombination. *Adv. Immunol.* **64,** 39–64 (1997).
8. Barnes, D. E., Stamp, G., Rosewell, I., Denzel, A. & Lindahl, T. Targeted disruption of the gene encoding DNA ligase IV leads to lethality in embryonic mice. *Curr. Biol.* **8,** 1395–1398 (1998).
9. Frank, K. M. *et al.* Late embryonic lethality and impaired V(D)J recombination in mice lacking DNA ligase IV. *Nature* **396,** 173–177 (1998).
10. Gu, Y. *et al.* Defective embryonic neurogenesis in Ku, but not DNA-PKcs, deficient mice. *Proc. Natl Acad. Sci. USA* **97,** 2668–2673 (2000).
11. Jiang, D., Lenardo, M. J. & Zuniga-Pflucker, C. p53 prevents maturation to the CD4+CD8+ stage of thymocyte differentiation in the absence of T-cell receptor rearrangement. *J. Exp. Med.* **183,** 1923–1928 (1996).
12. Guidos, C. J. *et al.* V(D)J recombination activates a p53-dependent DNA damage checkpoint in scid lymphocyte precursors. *Genes Dev.* **10,** 2038–2054 (1996).
13. Bogue, M. A., Zhu, C., Aguilar-Cordova, E., Donehower, L. A. & Roth, D. B. p53 is required for both radiation-induced differentiation and rescue of V(D)J rearrangement in scid mouse thymocytes. *Genes Dev.* **10,** 553–565 (1996).
14. Liyanage, M. *et al.* Multicolour spectral karyotyping of mouse chromosomes. *Nature Genet.* **14,** 312–315 (1996).
15. Karanjawala, Z. E., Grawunder, U., Hsieh, C. L. & Lieber, M. R. The nonhomologous DNA end joining pathway is important for chromosome stability in primary fibroblasts. *Curr. Biol.* **9,** 1501–1504 (1999).
16. Paulson, T. G., Almasan, A., Brody, L. L. & Wahl, G. M. Gene amplification in a p53-deficient cell line requires cell cycle progression under conditions that generate DNA breakage. *Mol. Cell. Biol.* **18,** 3089–3100 (1998).
17. Vanasse, G. J. *et al.* Genetic pathway to recurrent chromosome translocations in murine lymphoma involves V(D)J recombinase. *J. Clin. Invest.* **103,** 1669–1675 (1999).
18. Liao, M. J. *et al.* No requirement for V(D)J recombination in p53-deficient thymic lymphoma. *Mol. Cell. Biol.* **18,** 3495–3501 (1998).
19. Nacht, M. *et al.* Mutations in the p53 and SCID genes cooperate in tumorigenesis. *Genes Dev.* **10,** 2055–2066 (1996).
20. Rabbitts, T. H. Chromosomal translocations in human cancer. *Nature* **372,** 143–149 (1994).
21. Malynn, B. A. *et al.* The scid defect affects the final step of the immunoglobulin VDJ recombinase mechanism. *Cell* **54,** 453–460 (1988).
22. Hiom, K., Melek, M. & Gellert, M. DNA transposition by the RAG1 and RAG2 proteins: a possible source of oncogenic translocations. *Cell* **94,** 463–470 (1998).
23. Agrawal, A., Eastman, Q. M. & Schatz, D. G. Transposition mediated by RAG1 and RAG2 and its implications for the evolution of the immune system. *Nature* **394,** 744–751 (1998).
24. Jacks, T. *et al.* Tumor spectrum analysis in p53-mutant mice. *Curr. Biol.* **4,** 1–7 (1994).
25. Bieche, I. *et al.* Novel approach to quantitative polymerase chain reaction using real- time detection: application to the detection of gene amplification in breast cancer. *Int. J. Cancer* **78,** 661–666 (1998).

Acknowledgements

This work was supported by National Institutes of Health grants and a Hood Foundation grant (J.P.M.). J.S. is the Richard D. Frisbee III Foundation Fellow of the Leukaemia Society of America. Y.G. is an associate of the Howard Hughes Medical Institute. R.A.D. is an American Cancer Society research professor. F.W.A. is an investigator of the Howard Hughes Medical Institute.

Correspondence and requests for materials should be addressed to F.W.A. (e-mail: alt@rascal.med.harvard.edu).